Science of the Total Environment 959 (2025) 178010

Contents lists available at ScienceDirect

Science of the Total Environment

journal homepage: www.elsevier.com/locate/scitotenv

Portable emissions toxicity system: Evaluating the toxicity of emissions or polluted air by exposure of cell cultures at air-liquid interface in a compact field-deployable setup

Michal Vojtisek-Lom [a,*], Lubos Dittrich [a], Martin Pechout [a,b], Tereza Cervena [c], Anezka Vimrova [c], Jitka Sikorova [c], Tana Zavodna [c], Jakub Ondracek [d], Päivi Aakko-Saksa [e], Jan Topinka [c], Pavel Rössner [c]

[a] Faculty of Mechatronics and Interdisciplinary Studies, Technical University of Liberec, 46117, Czech Republic
[b] Department of Vehicles and Ground Transport, Technical Faculty, Czech University of Life Sciences, 165 00 Prague 6, Czech Republic
[c] Institute of Experimental Medicine of the Czech Academy of Sciences, Videnska 1084, Prague 4, Czech Republic
[d] Institute of Chemical Process Fundamentals of the Czech Academy of Sciences, Rozvojová 135, 165 00 Prague 6, Czech Republic
[e] VTT Technical Research Centre of Finland, Espoo 02150, Finland

HIGHLIGHTS

- Portable emissions toxicity system to study toxic effects of polluted air in field
- Cell cultures grown at air-liquid interface placed in sealed exposure boxes
- Incubator with exposure boxes placed in a vehicle for exposure to air or diluted exhaust
- Compact mobile setup for field studies, exposures up to 5 days, 4 h/day

GRAPHICAL ABSTRACT

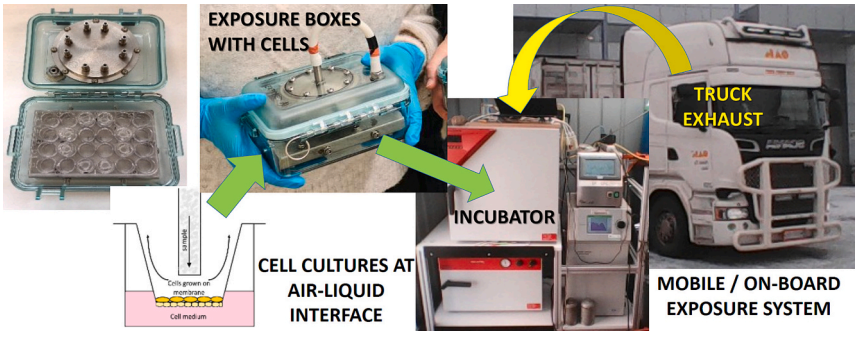

ARTICLE INFO

Editor: Anastasia Paschalidou

Keywords:
Air-liquid interface
Toxicity
Polluted air
Mobile sources
Mobile laboratory

ABSTRACT

Exposure of cell cultures at air-liquid interface (ALI), mimicking i.e. human lung surface, is believed to be one of the most realistic means to model toxicity of complex mixtures of pollutants on human health. The complexity of the close cooperation of "emissions source" and toxicology groups and of the instrumentation are among the limiting factors of ALI. In this work, the concepts of ALI exposure and real-world emissions monitoring using portable emissions monitoring systems (PEMS) are combined into a portable emissions or air toxicity system, for field deployment, including operation in moving vehicles. Cell cultures grown on 6 mm inserts are placed in an airtight 17x13x9 cm exposure box, where the sample is symmetrically distributed into 8 wells of a standard Transwell 24-well holder at 25 cm^3/min/insert. In a 40x35x45 cm inner dimensions incubator, sample and control air are conditioned to 5 % CO_2, 37 °C and >85 % humidity and drawn through 2–4 exposure boxes. Characterization with silver nanoparticles revealed 50 % particle losses at 15 nm and deposition rate of

* Corresponding author.
E-mail address: michal.vojtisek@tul.cz (M. Vojtisek-Lom).

https://doi.org/10.1016/j.scitotenv.2024.178010
Received 9 October 2024; Received in revised form 28 November 2024; Accepted 6 December 2024
Available online 21 December 2024

approximately 1.5 % at both 10 and 21 nm mean diameter. The system has undergone an extensive field validation, including 4 h of exposure and 2 h transport in a vehicle each day for 5 days, 5-day operation outside in vans and tents at −7 to +32 °C, long transport and test on a heavy-duty truck, during which cells were exposed to the diluted exhaust from the truck, this being the first known use of ALI exposure chamber as PEMS. The portable exposure chamber, along with a field-deployable auxiliary mobile base including a small laminar flow box, additional incubator and freezer, can be easily used to study the toxicity of various emissions, effluents and polluted air, aiming for a more relevant toxicity measure than chemical composition alone.

1. Introduction

Exposure to polluted air is one of the leading environmental risks and is among the top ten causes of premature death (HEI, 2024; Fuller et al., 2022; Pozzer et al., 2023; WHO, 2021). Most of the effects are currently associated with particulate matter (PM), chemical compounds bound to it, and reactive nitrogen species (Lelieveld et al., 2023), both directly emitted (primary emissions) and formed in the atmosphere at a later stage (secondary emissions), and tropospheric ozone formed under the presence of organic species, nitrogen oxides and sunlight. PM is typically assessed as its total mass, however, in reality, it varies in size, morphology, composition, toxicity and other adverse health effects. Nanoparticles (NP), with diameter < 100 nm, are produced primarily by combustion, followed by condensation of precursors at high temperature. NP have been reported to translocate to brain via the olfactory nerve (Elder et al., 2006; Oberdörster et al., 2004) and are known to efficiently deposit in human lung alveoli (Künzli et al., 2000), where they can interfere with gas exchange between inhaled air and blood (Almetwally et al., 2020), while the ultrafine fraction enters individual cells including subcellular structures and can be distributed to distant tissues and organs via blood stream. Carbonaceous particles from engines are more hazardous, on the equivalent mass basis, than "average" particles in the air (Krzyzanowski et al., 2005), and reduction of diesel particulate matter has been found to be, on a mass equivalent bases, 4–9 times more beneficial than the reduction in overall PM2.5 concentrations (Janssen et al., 2011). Other sources, like brake wear emissions, commercial aviation jet engine emissions, emissions from household stoves, welding, 3D printing, manufacturing, handling and processing of nanomaterials, and other novel technologies, are of emerging interest and concern. To further exacerbate the danger, NP are typically released in highly populated areas.

As a complement to chemical and physical analyses, in vitro toxicity tests using isolated DNA, cell cultures (Lawal et al., 2015; Libalova et al., 2016; Zhang and Balasubramanian, 2014) and animal lung tissue slices (Bion et al., 2002; Morin et al., 1999) have been carried out. Various experimental models cell cultures have been exposed to previously collected and resuspended particulate matter (Rothen-Rutishauser et al., 2008; Gerlofs-Nijland et al., 2013; Ghio et al., 2013; Martin et al., 2017; Totlandsdal et al., 2015).

Air-liquid interfaces (ALI), where cell cultures supported in media on one side are exposed in real time to a mixture of pollutants (Aufderheide and Mohr, 1999; Savi et al., 2008) were developed as a physiologically relevant alternative to standard in vitro tests (Geiser and Lang, 2007; Lacroix et al., 2018; Steiner et al., 2014), and used with diluted fresh vehicle exhaust (Hawley et al., 2014; Oeder et al., 2023; Müller et al., 2010; Steiner et al., 2012 and 2015). A review of ALI exposure systems is given in previous work (Rössner et al., 2021a), a review of models is given in Upadhyay and Palmberg (2018). Such in vitro toxicity tests may provide a more representative assessment than the one based on chemical composition alone, yet avoid ethically problematic, and not necessarily more representative, animal studies (Anadón et al., 2014).

Smaller particles and gaseous compounds are deposited by diffusion, with deposition rates reported roughly around 2 % (Bitterle et al., 2006; Rothen-Rutishauser et al., 2008; Tippe et al., 2002). In some cases, the deposition rate of particles, but obviously not gaseous compounds, is increased by electrostatic charging of the particles (Aufderheide et al., 2003; Geiser et al., 2017; Zavala et al., 2014), by thermophoretic deposition (Ihalainen et al., 2018), or by inertial impaction (Cooney and Hickey, 2011). While thermophoresis effects are not overly dependent on particle size, the particle charge distribution, as well as probability of deposition by impaction, depends on the particle size. Enhanced deposition of particles, but not gases, raises the issue of how representative such exposure is in cases where the gaseous fraction can contribute significantly to the toxic effects. For example, in diesel exhaust, the cellular response (interleukin-8 secretion) was about equally divided between gaseous fraction (filtered exhaust) and semi-volatile fraction of particles (Holder et al., 2007). In exposures where both gaseous pollutants and aerosols were considered, no deposition enhancement has been used (Binder et al., 2022; Guénette et al., 2022).

The use of ALI has grown considerably over the last decade, with a variety of cultures on a varying number of 6 mm, 12 mm and 24 mm inserts, typically kept at 37°C, humidification of the sample, with our without addition of CO_2, with deposition enhancement by particle charging or with deposition by diffusion, and exposure times of tens of minutes to 2 h, using a mix of commercially available and in-house fabricated systems (Rössner et al., 2021b; Guénette et al., 2022; Hakkarainen et al., 2022; Buckley et al., 2024).

As far as practical application of ALI interfaces, their operation in the field is not necessarily simple, due to both the necessity of a close cooperation between the toxicology team and the team providing the sample from the studied process or environment, and due to the necessity to have a toxicological laboratory nearby, with at least some facility at the testing site. These factors, in the opinion of the authors, impose, along with the inherent complexity and expense of toxicological assays, practical limits hindering ALI exposure applications.

The aim of this work was to develop and validate the concept of a simple, practical, compact, portable ALI exposure system suitable for field studies of a range of sources of complex mixtures of air pollutants, together with an easily transportable auxiliary toxicological laboratory that can be deployed in the field without a readily access to laboratory equipment and sometimes not even to the basic amenities.

2. Experimental design and methods

2.1. Portable exposure box

The cell cultures are housed in commonly used commercial 24-well Transwell™ plates, out of which 8 positions are populated with 6 mm diameter membrane wells (inserts) with cell cultures placed in supporting media. The plate sits on an adjustable stainless steel slab placed in a modified waterproof camera box (exposure box). The sample is delivered by a symmetrical stainless steel distributor mounted in the lid of the box into 8 nozzles, each of 5 mm outer diameter and inner diameter increasing from a 1 mm restrictor equalizing the flow to 25 cm^3/min for each nozzle to 4 mm at the exit plane located 1–2 mm above the membrane with the cell culture. The 17x13x9 cm exposure boxes, shown in Fig. 1, can be hermetically sealed by connecting the inlet and the outlet with a flexible tubing, and are stored and transported this way in an insulated box or in an incubator.

2.2. Toxicological incubator (exposure chamber)

Up to four exposure boxes can be used for exposure in a modified small 40x35x45 cm inner dimensions commercial incubator (Binder BF56, Tuttlingen, Germany). The exposure boxes are sealed, so the only role of the incubator is to provide a stable temperature of 37 °C. In two parallel branches for the sample examined and synthetic air (or purified ambient air) used as control, food-grade CO_2 is added to the sample at 5 % by volume, and the sample passes first through a heat exchanger and then through a Nafion membrane humidifier (MH-110-12S-2, Permapure) filled with deionized water to increase its temperature to 37 °C and relative humidity to 85–95 %, and then it is directed to the inlet of one or more exposure boxes. From the outlet of each exposure box, the sample is drawn through a filter, a rotameter, and a miniature rotary vane pump with an in-house variable speed drive. The schematic and photo of the setup are shown in Fig. 2. The incubator was tested at temperatures of −5 °C to its practical limit of +33 °C, with electric power consumption of the entire setup below 100 W at 20–25°C plus approximately 3 W for each °C below 20°C. The entire system weighs 39 kg and is self-contained, except for separate bottles with CO_2 and, if used, compressed control air and auxiliary power source (battery pack and inverter).

2.3. Auxiliary equipment

For short trips to the exposure site (lasting a maximum of a couple of hours), the exposure boxes can be sealed with a CO_2-enriched atmosphere and transported in an insulated polystyrene box containing preheated pads. Upon arrival, they can be directly connected to either the control or sample line. For longer trips, the presence of additional equipment at or near the exposure place is required. This includes a laminar flow box, which circulates filtered air to provide a reasonably sterile work environment for processing cell cultures, a small cell incubator to maintain live cells, a small freezer to store samples and necessary chemicals, a microscope, and cell culture supplies. Example photographs of outdoor measurements conducted at ambient temperatures ranging from −7 °C to +32 °C (with 33–34 °C being the practical limit without active cooling to maintain the cell culture temperature of 37 °C) are shown in Fig. 3.

2.4. Physical characterization (particle depositions)

Particle losses in the sample conditioning train, up to the exposure box inlet, were characterized by alternate sampling of particles in parallel to the incubator inlet and in lieu of one exposure box by a condensation particle counter (CPC), alone or preceded by the scanning mobility particle sizer (SMPS). At the same time, other instruments were sampling in parallel with the incubator to ensure the stability of particle concentration and size distribution. Gasoline engine exhaust, metallic particles generated by spark ablation (VSP), and silver nanoparticles (AgNP) generated in a furnace were used, of which primarily AgNP are reported on here, with other tests being done on older, larger version of the chamber. In the experiment with AgNP, monodisperse aerosol generated by a furnace followed by an electrostatic classifier was introduced into the exposure chamber, two CPC (CPC3752, TSI) were used simultaneously and switched their positions at each point to compensate for possible differences between them. In other experiments, polydisperse Ag aerosol was fed into the chamber and one CPC was used, its location alternated between exposure box inlet and incubator inlet.

In the AgNP experiment, particle deposition rate was examined by placing 3 mm electron microscope grids on inserts in lieu of cell cultures, depositing monodisperse aerosols of 10 and 30 nm diameter for approximately 17 h and polydisperse aerosols with mean diameters of 11.0 and 20.1 nm, geometric standard deviations of 1.55 and 1.85, generated at 1100 °C and 1200 °C, respectively, for approximately 3 h, and determining the number of particles deposited and their size from transmission electron microscope (TEM) imaging.

2.5. Toxicological characterization

The exposure boxes are functionally the same as described in the previous work by the authors (Vojtisek-Lom et al., 2020), where they were used in a larger incubator where human lung cells (BEAS-2B, Rössner et al., 2021b), 3-D lung tissue models (Rössner Jr. et al., 2019), and human olfactory mucosa cells (Saveleva et al., 2024) were exposed to diluted exhaust from diesel and spark ignition engines running on a variety of biofuels. The longest exposures were twice day for 2 h for 5 consecutive days. The results of these previous studies are summarized in the Results section. In all combustion studies, both the dilution air and the combustion air provided to the engine in an engine laboratory are filtered and close to sterile. To extend the use of the exposure boxes to polluted indoor or outdoor air, additional exposures of cell cultures to outside air at a National Atmospheric Observatory Kosetice (NAOK, considered as a rural background station of the CR), not within the proximity of roads and industrial areas but amidst forests, pastures and agricultural crop areas, were made for 2 h, twice a day, for five consecutive days, for the purpose of assessing the effects of “common”, non-sterile air.

Fig. 1. Exposure box with a standard 24-well plate with 8 active 6-mm inserts.

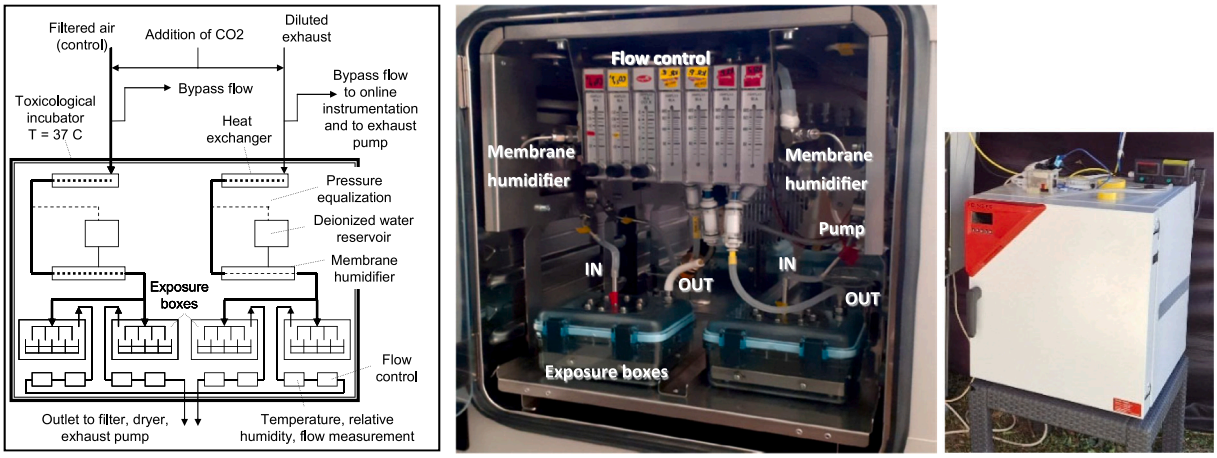

Fig. 2. Exposure chamber setup in a 45x40x35 inner dimensions incubator.

Fig. 3. Field installations of the exposure chamber and the auxiliary laboratory: a,f) laminar flow box placed in a tent; b) left to right: CO_2 and synthetic air bottles, particle counter (UF-CPC 200, Palas) and particle classifier (Engine Exhaust Particle Sizer, TSI), laminar flow box, exposure chamber; c,d) exposure chamber and particle counter and classifier in a 3 m × 2 m lockable garden house; e) winter tests with instruments in a van and air quality monitoring station trailer.

3. Results of validation and trial runs

3.1. Characterization of particle losses

The particle losses in the sample conditioning system, between the incubator inlet and the exposure box inlet, as determined for silver particles in nitrogen, are shown in Fig. 4a. The penetration rate increases with the particle size, nearly logarithmically (in a nearly linear manner with respect to the logarithm of the particle size) until about 25 nm, being roughly 25 % at 10 nm, 50 % at 15 nm and 70 % at 20 nm, plateauing at around 80 %. The error bars represent standard deviations which are relatively small. (Note: The standard deviation was computed from the standard deviations of values measured at each position with each of the two counters.)

Analogous results shown in Fig. 4b were obtained with a similar system but placed in a larger incubator with longer sample travel path, when tested with copper, iron and gold particles generated using a spark generator. The particle size range is determined by the particle sizer limit on the lower end (7 nm for Cu, 14 nm for Fe and Au, measurements were done during different campaigns) and by very low concentrations beyond 100 nm. There, the standard deviations are substantially higher, due to highly variable performance of the spark generator. It is the authors opinion that Au particles are the most representative, as the older ALI system (Vojtisek-Lom et al., 2020) had higher diffusion losses and therefore lower penetration rates.

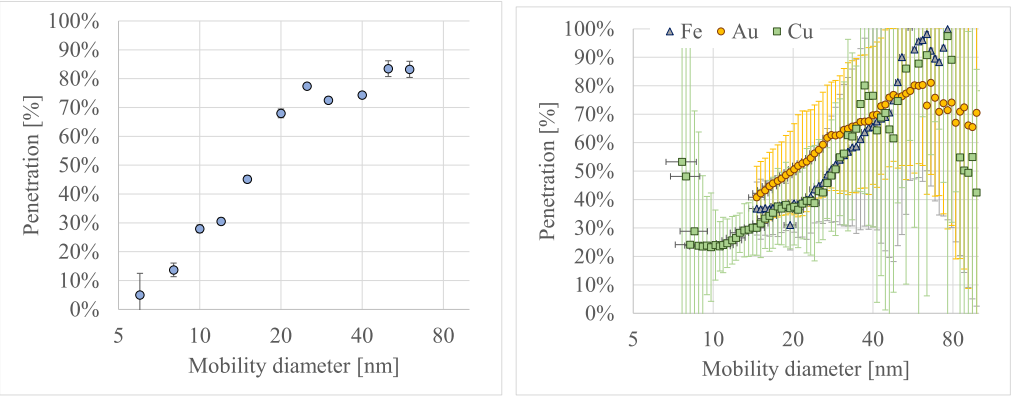

Fig. 4. Penetration rates for a) silver particles with this ALI exposure system and b) copper, iron and gold particles with previous ALI exposure system.

3.2. Particle deposition assessment

At 1100 °C, the number of particles deposited, determined from TEM images (left photo in Fig. 5) was in the range of 55–120 (mean 88) particles per 2.94 um^2 area, corresponding, at 6 mm insert diameter, 25 cm^3/min/insert and 161 min exposure time to mean concentrations of 2.06 10^5 particles deposited per cm^3 flown through the insert. At the same oven settings, the mean particle concentration measured by nanoSMPS (SMPS 3938, EC 3082, DMA 3085, CPC 3756, all TSI) was 1.24 10^7 #/cm^3, yielding a mean overall deposition efficiency of 1.66 %. Of 518 particles counted from a total of six TEM images, 256 were larger than 11 nm, which is consistent with the mean diameter of 11.0 nm measured by the nanoSMPS.

At 1200 °C, a large number of very small particles was observed (right photo in Fig. 5). Of 972 particles counted, 552 were smaller than 5 nm. On one of the six counting areas, 504 particles were counted, of which 372 were smaller than 5 nm. The remaining five counting areas had 57–107 particles per 2.94 um^2, of which 38–58 were larger than 5 nm and 16–29 were larger than 20 nm. Such a large number of very small particles, which were unlikely to be part of the test aerosol and even if so, which were unlikely to penetrate through the sampling system, was attributed to a fragmentation of larger clusters, albeit the mechanism of such fragmentation is not known to the authors. It is the opinion of the authors that only units of percent of large, 20 nm mean diameter, clusters were lost to <5 nm fragments. Assuming symmetrical particle size distribution, the total number of "original" (as generated) particles was roughly twice the number of >20 nm particles, which was 22 per 2.94 um^2, or 4.3 × 10^4 particles deposited per cm^3 flown through the insert. The deposition efficiency was therefore determined as 8.6 × 10^4 particles deposited per cm^3 divided by the mean concentration of 1.39 × 10^7 #/cm^3, or 0.62 %.

The actual deposition efficiency is likely higher due to particle clustering. In the original aerosol, only 2.34 % of all particles were larger than 40 nm, while among 132 deposited particles larger than 20 nm, 46 (35 %) were larger than 40 nm. At 2.55 fractal dimension (sintered but not spherical particles), particles larger than 40 nm constitute 70 % of the total mass, compared to particles larger than 40 nm constituting roughly a quarter of the total mass in the original distribution. Therefore, about 40 % of the deposited particle mass (30 % ≤ 40 nm and 10 % > 40 nm) corresponds to the original size distribution and about 60 % to non-original agglomerates. Given this, the deposition efficiency should be, in theory, higher by a factor of 2.5, or about 1.55 %. This calculation is, however, speculative, as toxicological effects are dependent on particle size, and do not necessarily correspond to any common physical metric.

Without assessing particle sizes, and counting all detectable particles, excluding one outlier frame with a high number of <5 nm particles, the deposition efficiency would be 1.19 %.

In theory, with an increasing size of incoming nanoparticles, the penetration rate increases mainly due to decreased diffusion losses in the sampling and conditioning system, but the "insert" deposition efficiency (ratio of particles deposited to particles entering the insert) decreases due to lower diffusion rate of larger particles. The product of the penetration and deposition rates, or the overall deposition rate, is the

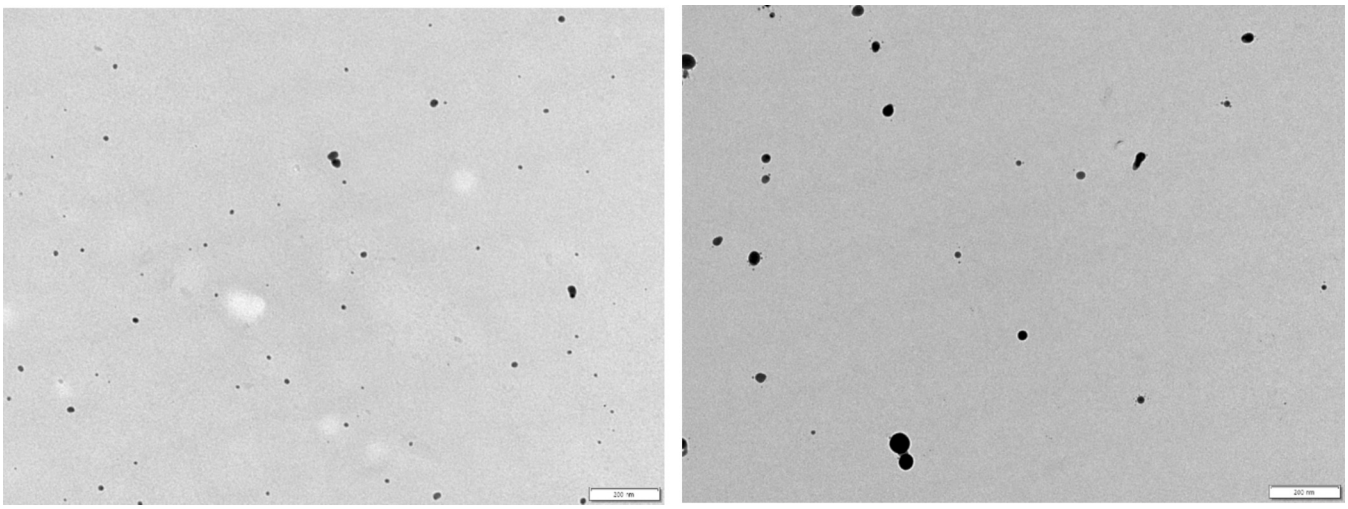

Fig. 5. Deposition of polydisperse silver particles of a) 11 nm and b) 20 nm mean diameter onto electron microscope grid placed on inserts.

resulting fraction of particles deposited is the product of penetration rate, and its dependency on particle size may not be straightforward. Here, increasing particle humidity, a necessary step at ALI interfaces, may also, at least temporarily, affect the particle size. Also, the rather high concentrations of 10^7 #/cm^3, chosen to get a detectable amount of particles in a reasonable time, favors particle coagulation and agglomeration.

Given the uncertainties involved, the reported deposition rate of 1.65 % for 11 nm aerosol and the estimated deposition rate of 1.55 % for 20 nm aerosol, interpreted as the fraction of particles entering the incubator that in some form are deposited on the insert surface, are more of a rough estimate than a specification, expected to vary among the source aerosols, notably considering the effects of the humidification process. Taking the pragmatic approach, the authors believe that a deposition rate of somewhere in the range of 1–2 % for silver particles with a mean diameter of 11 nm (the smallest the authors were confident to produce in meaningful quantities, to deposit, and to analyze), is a reasonable proof of the validity of the concept.

3.3. Cytotoxicity effects of common air

Fig. 6 presents the results of a trial cytotoxicity assay (LDH; lactate dehydrogenase) after 5 days of exposure to outdoor air. Up to four sample types, representing different types of cells, were utilized: hOM (human olfactory mucosa cells), MucilAir Healthy (a 3D cell model derived from healthy donors). Cells were exposed to ambient air for 2 h, followed by a 2-h period without airflow, and then subjected to another 2 h of exposure. This cycle was repeated daily over 5 days (time points T1 – T5, starting at T0). After each day, cells were kept overnight in a cell incubator, and the culture medium was collected for LDH analysis. LDH release was normalized to the T0 time point to account for differences in the baseline metabolic activity of the cell types. Even though for some samples we observed elevated cytotoxicity values over time, it is important to note that the cytotoxicity levels mostly did not exceed established limits (> 80 %), indicating that the cells remained within a tolerable range of stress. Overall, the cells were in good shape throughout the experiment. Importantly, no contamination was observed during the experimental period, as the cells were cultured with antibiotics and antimycotics due to the in vitro system's lack of an immune system, ensuring the reliability and integrity of the results.

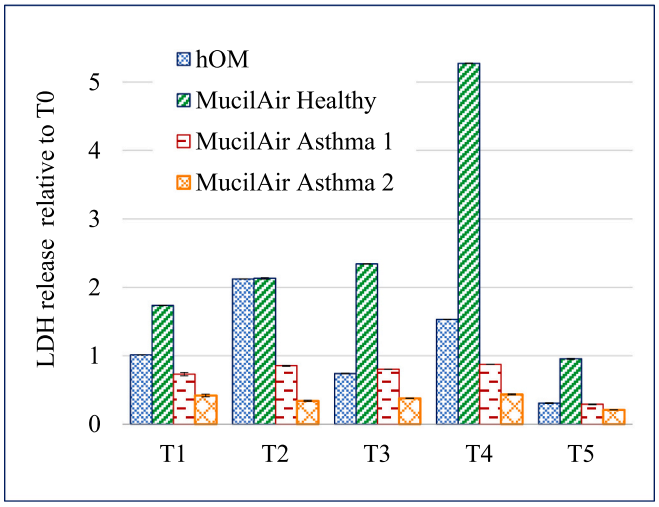

Fig. 6. Cytotoxicity results from trial 5 day exposure: Four samples (hOM, MucilAir Healthy, MucilAir Asthma 1, MucilAir Asthma 2), representing three types of cells were exposed repeatedly for 5 days to ambient air for 2 h twice a day. LDH release – ratio of absorbance to that at T0 – is shown at the end of each day.
Details on exposure are provided in the Cytotoxicity effects of common air section.
*hOM (human olfactory mucosa cells); MucilAir Healthy (3D cell model from healthy donor); MucilAir Asthma (3D cell model from asthmatic donor).

4. Discussion

4.1. Laboratory and field campaigns

In the predecessor of this system (Vojtisek-Lom et al., 2020), BEAS-2B cell line was exposed to gasoline exhaust fumes for 1–2 h at room temperature (RT), with results published in several studies between 2019 and 2021 (Rössner Jr. et al., 2019; Cervena et al., 2020; Rössner et al., 2021b). Similarly, the 3D Lung Model (MucilAir) was subjected to gasoline and diesel exhaust fumes, with exposure durations of 1-2 h at RT. While some findings have been published (Rössner Jr. et al., 2019; Cervena et al., 2020), others remain unpublished. Human Olfactory Mucosa Cells (hOM) were exposed to diesel exhaust fumes for 1 h at RT (Saveleva et al., 2024). The A549 co-culture with THP-1 underwent exposure to spark ablation nanoparticles for 1 h at RT. During some of these studies, the exposure boxes have been prepared in an ordinary toxicological laboratory and then transported to and from the exposure site by car (1 h drive each way) and by sled (in an insulated box, approx. 10-min ride on ice in Finland).

In the system presented here, the A549 co-culture with THP-1 and hOM were exposed to ambient air for 4 h for 5 consecutive days at temperatures ranging from −7 °C to +32 °C. During this time, the exposure chamber has been operated in a van (low temperatures), in a lockable metal garden shed, in an exhibition tent (higher temperatures), and in general office spaces, along with online particle monitoring instrumentation. The entire setup has been powered both from the grid and by batteries and inverter (5 kWh LiFePo batteries and 2 kW inverter/charger in a 50 kg package, however, most of this capacity was used by online instrumentation). Its placement in heated or air conditioned environments, typical for field campaigns with instruments in a van or in a container, would most likely extend the operating range, however, such conditions are representative of human exposure only in a small number of cases.

The exposure chamber and the auxiliary equipment has been transported by an ordinary van to different campaigns, the longest distance being from Prague to Tampere, Finland.

Table 1 summarizes research that highlights the use of our in-house exposure system. This summary underscores the pivotal role of our custom-built exposure system in facilitating these studies, reflecting

Table 1
An overview of experiments conducted on various cell types exposed to different environmental conditions, detailing the exposure type, duration, temperature, and publication status using our exposure system (Vojtisek-Lom et al., 2020).

Cell type	Exposure	Duration	°C	Published in
BEAS-2B	Gasoline exhaust fumes	1–2 h	RT	Rössner Jr. et al., 2019; Cervena et al., 2020; Rössner et al., 2021b
3D lung model (MucilAir)	Gasoline exhaust fumes	1–2 h	RT	Rössner Jr. et al., 2019; Cervena et al., 2020,
	Diesel exhaust fumes	1–2 h	RT	Not published
	Ambient air	4 h	−7 °C to +32 °C	Rössner et al., 2024
A549 coculture with THP-1	Spark ablation nanoparticles	1 h	RT	Not published
hOM (human olfactory mucosa cells)	Diesel exhaust fumes	1 h	RT	Saveleva et al., 2024
	Ambient air	4 h	−7 °C to +32 °C	Rössner et al., 2024

ongoing research and publication efforts on the biological impact of environmental exposures.

4.2. Effects of transport and handling during field campaigns on control cells

Our studies by Rössner Jr. et al. (2019) and Cervena et al. (2020) are part of a comprehensive investigation into the toxicological impacts of gasoline engine emissions on human airway models, utilizing both a 3D human airway model (MucilAir™) and human bronchial epithelial cells (BEAS-2B) grown at an air-liquid interface. In both studies, control cells played a critical role in establishing a baseline for understanding the effects of gasoline engine emissions on human airway models. The control cells, which were not exposed to gasoline exhaust, served as a reference to determine the normal, unstressed state of the human bronchial epithelial cells (BEAS-2B) and the 3D human airway model (MucilAir™). In the absence of exposure to harmful pollutants, these control cells maintained typical cellular morphology and function. They exhibited stable levels of reactive oxygen species (ROS), indicating that oxidative stress was minimal or absent under normal conditions. Furthermore, the control cells did not show signs of DNA damage, which is crucial as it underscores that any observed genotoxic effects in the exposed cells could be directly attributed to the emissions rather than any inherent cellular instability. Additionally, the control cells demonstrated a lack of significant inflammatory response, with cytokine levels such as IL-6 and IL-8 remaining at baseline levels. This absence of an inflammatory reaction in the control cells is particularly important as it highlights the inflammatory response seen in exposed cells as a direct consequence of the gasoline engine emissions. Upon exposure to gasoline emissions, a significant increase in oxidative stress markers was observed in both models, indicating that oxidative stress is a central mechanism of toxicity. This was accompanied by a pronounced inflammatory response, with elevated levels of pro-inflammatory cytokines such as IL-6 and IL-8. Additionally, both studies reported significant DNA damage, highlighting the genotoxic potential of these emissions. The 3D MucilAir™ model demonstrated greater resilience compared to the simpler BEAS-2B cells, underscoring the importance of using complex models for more accurate toxicological assessments.

4.3. On enhancing the deposition rate

The particle deposition rate observed here, roughly 1.5 %, and in line with about 1.5–2 % reported by Mülhopt et al. (2016) for diffusion-controlled systems, seems to be relatively low compared to systems that enhance particle deposition by thermophoretic effect (Broßell et al., 2013; Ihalainen et al., 2018) or by charging the particles and applying voltage on the order of hundreds to thousands of Volts on the cells to attract the charged particles (Savi et al., 2008; Aufderheide et al., 2003; Geiser et al., 2017). While the increase in deposition rate due to the thermophoretic effect is practically independent of particle size, the average number of charges on a particle is approximately proportional to the particle diameter (Hinds, 1999), and therefore, the deposition rate increases with the particle diameter. While such enhancement is useful for the study of aerosols, our system has been intended for studying complex mixtures including both aerosols and gaseous pollutants, where considerable portion of toxic effects can be associated with the gas phase. Therefore, we have opted not to enhance the particle deposition.

4.4. On the choice of the flow rate

The particle losses due to diffusion, the dominant mechanism of loss of nanoparticles in the sampling system, increase with the residence time, and therefore favor higher flow rates. Higher flow rates, on the other hand, increase the stress on the cell cultures, leading to higher cytotoxicity as assessed by LDH release (Buckley et al., 2024).

The absolute particle deposition rate (number of particles deposited on the cell culture) is, in our opinion, very little affected by the flow rate. The number of particles delivered to the cell cultures is proportional to the flow, but at the same time, the probability of particle deposition by diffusion is proportional to the residence time, which is inversely proportional to the flow rate. Therefore, the absolute deposition rate, a product of deposition efficiency and the total number of particles introduced into the system, is relatively constant. Buckley et al. (2024) reported a deposition rate of silver NP on 6 mm inserts of approximately 5–10 % (five times the rate observed here), but at 5 ml/min flow (one fifth of that used in this study).

4.5. Comparison of the deposition rate to that in human lung alveoli

Despite the relatively low deposition rate, the particle deposition is, in our opinion, higher, per surface area, compared to human lungs, as demonstrated in the following calculation.

At 10^4 particles/cm^3, a reasonable street ambient air value, 25 cm^3/min flow, and 20 h total exposure time, 3×10^8 particles pass by the 6 mm diameter insert area. At 1 % deposition efficiency, about 10^5 particles per mm^2 are deposited. If the same aerosol is inhaled at 12 dm^3/min for 20 h, at human lung surface area of 78 m^2 (Guha et al., 2014), a reasonable value within (not counting the extremes) the roughly 30–100 m^2 reported range, reviewed in (Fröhlich et al., 2016), about 2×10^3 particles per mm^2 surface area enter the lungs. The deposition rate, different for different regions of the lung, varies with particle size, with a peak of alveolar deposition efficiency of about one half at roughly 10–20 nm (Hofmann, 2009), a size comparable to where peak concentrations in urban areas were observed by Stolcpartova et al. (2015). A deposition rate of 32–73 % for common household sources was reported by Vu et al. (2017). At 50 % deposition efficiency, about 1000 particles/mm^2 are deposited in human lungs over a 20-hour exposure to 10^4 #/cm^3, two orders of magnitude less compared to the exposure boxes. It should be noted that while the absolute deposition efficiency in human lung is larger than in the exposure chamber, the deposition efficiency per surface area of lung or culture is about two orders of magnitude higher for the exposure box than for a lung. Therefore, for human lung air-liquid interface, the 20-h exposure corresponds to a human exposure on the order of hundred times higher - months to a year at units of hours per day.

4.6. Use of ALI exposure systems as PEMS

The exposure chamber has been transported on two instrumented heavy-duty trucks while sampling their diluted exhaust and exposing the cell cultures to it. This study was, to our knowledge, the first time ALI exposure was used on board a moving vehicle to sample its emissions, analogous to PEMS. As no online measurement is taking place, a logical analogous acronym Portable Emissions Toxicity System (PETS) is suggested.

The size, power consumption and operation of the exposure chamber is well in line with Fourier Transform Infra Red (FTIR) spectrometers, tunable diode laser spectrometers, and other instruments used as portable emissions monitoring systems (PEMS), evaluating a range of compounds for research, and lately also regulatory, purposes. While by traditional characterization of aerosol instrument by Hallquist et al. (2009) by their ability to resolve chemical composition, an ALI exposure system might be considered a “useless instrument” as it does not provide any chemical characterization, in complex mixtures, where considerable portion of toxic effects is associated with a very small fraction of the mixture by mass, a more direct assessment of toxicity is, in our opinion, a valuable tool, due to complex and often unknown positive and negative synergies among the different compounds. There were no observable adverse effects of the transport on the control cells, and neither there were any observable adverse effects on control cells which were transported by vehicle in exposure boxes (without being exposed to exhaust) in several of our studies. Therefore, we believe that the ALI exposure

developed here can be relatively easily replicated by other laboratories and used to evaluate the effects of exhaust from novel fuels and propulsion systems, as well as a range of real-world pollutant mixtures, such as emissions from ships, airplanes, wood stoves, welding and metal working operations, industrial plants, nanomaterial production and handling plants, and similar operations during which complex mixtures with potentially adverse inhalation risks to human health are produced.

5. Conclusions

A portable toxicological incubator in which cell cultures are exposed to pollutant mixtures at air-liquid interface, intended for practical field use, has been developed and tested in the field. Eight 6 mm inserts with cell cultures are contained in airtight exposure boxes which can be easily transported and handled in the field, and placed in a portable incubator during the exposure. There, the sample stream and the control stream (i.e., synthetic air), conditioned to 37 °C, 5 % CO_2 and > 85 % relative humidity, are introduced at 25 cm^3/min/insert into exposure boxes containing sample and control cell cultures, which in our studies were MucilAir™ 3-D human lung models, human olfactory mucosa cells, and BEAS-2B and A549 human lung cells. Exposures up to five days, twice two hours per day, to diluted exhaust and outdoor ai have been performed, with no noticeable adverse effects to control cells due to biological air contaminants or due to extensive transport of the cells either during or before/after the exposure. The exposure system has been mounted on a moving heavy-duty truck in northern Finland, sampling its diluted exhaust, this being the first use of an ALI exposure system as a part of an on-board vehicle emissions monitoring system.

A field laboratory, including particle monitoring instruments, batteries, and laminar flow box for cell handling has been deployed for one-week campaigns in a van, a tent and a garden shed at outdoor temperatures from −7 °C to +32 °C, demonstrating the feasibility of ALI exposure in field conditions. The approach developed here can easily be replicated by other labs and can be used for practical assessment of toxicity of complex mixtures from a variety of sources.

CRediT authorship contribution statement

Michal Vojtisek-Lom: Writing – original draft, Visualization, Validation, Supervision, Project administration, Methodology, Investigation, Funding acquisition, Formal analysis, Data curation, Conceptualization. **Lubos Dittrich:** Methodology, Conceptualization. **Martin Pechout:** Methodology, Investigation. **Tereza Cervena:** Writing – original draft, Investigation, Data curation. **Anezka Vimrova:** Investigation. **Jitka Sikorova:** Investigation, Data curation. **Tana Zavodna:** Investigation, Data curation. **Jakub Ondracek:** Validation, Investigation. **Päivi Aakko-Saksa:** Supervision, Funding acquisition. **Jan Topinka:** Writing – original draft, Supervision, Project administration, Funding acquisition. **Pavel Rössner:** Writing – original draft, Supervision, Project administration, Methodology, Funding acquisition.

Funding

The on-road truck study was part of the PAREMPI project, funded by the European Commission within the Horizon Europe programme, grant no. 101096133. All other parts of this work have been funded by the Czech Science Foundation grant no. 22-10279S: The impact of real-world ambient air pollution exposure on human lung and olfactory cells grown at the air-liquid interface. The particle calibration laboratory and part of the toxicological laboratory instruments, other than the exposure system, were funded by the Czech Ministry of Education large research infrastructure projects no. LM2023030 (ACTRIS-CZ), LM2023066 (NanoEnviCz) and LM2023053 (EATRIS-CZ).

Declaration of competing interest

The authors declare the following financial interests/personal relationships which may be considered as potential competing interests:

Michal Vojtisek-Lom reports financial support was provided by Czech Science Foundation. Jan Topinka reports financial support was provided by Horizon Europe. If there are other authors, they declare that they have no known competing financial interests or personal relationships that could have appeared to influence the work reported in this paper.

Data availability

Data will be made available on request.

References

Almetwally, A.A., Bin-Jumah, M., Allam, A.A., 2020. Ambient air pollution and its influence on human health and welfare: an overview. Environ. Sci. Pollut. Res. Int. 27 (20), 24815–24830. https://doi.org/10.1007/s11356-020-09042-2.

Anadón, A., Martínez, M.A., Castellano, V., Martínez-Larrañaga, M.R., 2014. The role of in vitro methods as alternatives to animals in toxicity testing. Expert Opin. Drug Metab. Toxicol. 10 (1), 67–79.

Aufderheide, M., Mohr, U., 1999. CULTEX a new system and technique for the cultivation and exposure of cells at the air/liquid interface. Exp. Toxicol. Pathol. 51 (6), 489–490. https://doi.org/10.1016/S0940-2993(99)80121-3.

Aufderheide, M., Knebel, J.W., Ritter, D., 2003. Novel approaches for studying pulmonary toxicity in vitro. Toxicol. Lett. 140-141, 205–211. https://doi.org/10.1016/S0378-4274(02)00512-X.

Binder, S., Rastak, N., Karg, E., Huber, A., Kuhn, E., Dragan, G.C., Monsé, C., Breuer, D., Di Bucchianico, S., Delaval, M.N., et al., 2022. Construction of an in vitro air–liquid interface exposure system to assess the toxicological impact of gas and particle phase of semi-volatile organic compounds. Toxics 10, 730. https://doi.org/10.3390/toxics10120730X.

Bion, A., Fall, M., Gouriou, F., Le Prier, E., Dionnet, F., Morin, J.P., 2002. Biphasic culture of rat lung slices for pharmacotoxicological evaluation of complex atmospheres. Cell Biol. Toxicol. 18 (5), 301–314. https://doi.org/10.1023/a:1019544416969.

Bitterle, E., Karg, E., Schroeppel, A., Kreyling, W.G., Tippe, A., Ferron, G.A., Schmid, O., Heyder, J., Maier, K.L., Hofer, T., 2006. Dose-controlled exposure of A549 epithelial cells at the air-liquid interface to airborne ultrafine carbonaceous particles. Chemosphere 65 (10), 1784–1790. https://doi.org/10.1016/j.chemosphere.2006.04.035.

Broßell, D., Tröller, S., Dziurowitz, N., Plitzko, S., Linsel, G., Asbach, C., Azong-Wara, N., Fissan, H., Schmidt-Ott, A., 2013. A thermal precipitator for the deposition of airborne nanoparticles onto living cells—rationale and development. J. Aerosol Sci. 63, 75–86. https://doi.org/10.1016/j.jaerosci.2013.04.012.

Buckley, A., Guo, C., Laycock, A., Cui, X., Belinga-Desaunay-Nault, M.F., Valsami-Jones, E., Smith, R., 2024. Aerosol exposure at air-liquid-interface (AE-ALI) in vitro toxicity system characterisation: particle deposition and the importance of air control responses. Toxicol. In Vitro 100, 105889.

Cervena, T., Vojtisek-Lom, M., Vrbova, K., Ambroz, A., Novakova, Z., Elzeinova, F., Sima, M., Beranek, V., Pechout, M., Macoun, D., Klema, J., Rossnerova, A., Ciganek, M., Topinka, J., Rossner Jr., P., 2020. Ordinary gasoline emissions induce a toxic response in bronchial cells grown at air-liquid interface. Int. J. Mol. Sci. 22 (1), 79. https://doi.org/10.3390/ijms22010079.

Cooney, D.J., Hickey, A.J., 2011. Cellular response to the deposition of diesel exhaust particle aerosols onto human lung cells grown at the air–liquid interface by inertial impaction. Toxicol. In Vitro 25 (8), 1953–1965. https://doi.org/10.1016/j.tiv.2011.06.019.

Elder, A., Gelein, R., Silva, V., Feikert, T., Opanashuk, L., Carter, J., Potter, R., Maynard, A., Ito, Y., Finkelstein, J., Oberdörster, G., 2006. Translocation of inhaled ultrafine manganese oxide particles to the central nervous system. Environ. Health Perspect. 114 (8), 1172–1178. https://doi.org/10.1289/ehp.9030.

Fröhlich, E., Mercuri, A., Wu, S., Salar-Behzadi, S., 2016. Measurements of deposition, lung surface area and lung fluid for simulation of inhaled compounds. Front. Pharmacol. 7, 181. https://doi.org/10.3389/fphar.2016.00181.

Fuller, R., Landrigan, P.J., Balakrishnan, K., et al., 2022. Pollution and health: a progress update. Lancet. Planet. Health 6 (6), e535–e547. https://doi.org/10.1016/S2542-5196(22)00090-0.

Geiser, M., Lang, D., 2007. In vitro replica of the inner surface of the lungs for the study of particle-cell interactions. Altex 24, 82–84.

Geiser, M., Jeannet, N., Fierz, M., Burtscher, H., 2017. Evaluating adverse effects of inhaled nanoparticles by realistic in vitro technology. Nanomaterials 7 (2), 49. https://doi.org/10.3390/nano7020049.

Gerlofs-Nijland, M.E., Totlandsdal, A.I., Tzamkiozis, T., Leseman, D.L., Samaras, Z., Låg, M., Schwarze, P., Ntziachristos, L., Cassee, F.R., 2013. Cell toxicity and oxidative potential of engine exhaust particles: impact of using particulate filter or biodiesel fuel blend. Environ. Sci. Technol. 47 (11), 5931–5938. https://doi.org/10.1021/es305330y.

Ghio, A.J., Dailey, L.A., Soukup, J.M., Stonehuerner, J., Richards, J.H., Devlin, R.B., 2013. Growth of human bronchial epithelial cells at an air-liquid interface alters the response to particle exposure. Part. Fibre Toxicol. 10, 25. https://doi.org/10.1186/1743-8977-10-25.

Guénette, J., Breznan, D., Thomson, E.M., 2022. Establishing an air-liquid interface exposure system for exposure of lung cells to gases. Inhal. Toxicol. 34 (3–4), 80–89. https://doi.org/10.1080/08958378.2022.2039332.

Guha, S., Hariharan, P., Myers, M.R., 2014. Enhancement of ICRP's lung deposition model for pathogenic bioaerosols. Aerosol Sci. Tech. 48 (12), 1226–1235. https://doi.org/10.1080/02786826.2014.975334.

Hakkarainen, H., Salo, L., Mikkonen, S., Saarikoski, S., Aurela, M., Teinilä, K., Jalava, P. I., 2022. Black carbon toxicity dependence on particle coating: Measurements with a novel cell exposure method. Sci. Total Environ. 838, 156543. https://doi.org/10.1016/j.scitotenv.2022.156543.

Hallquist, M., Wenger, J.C., Baltensperger, U., Rudich, Y., Simpson, D., Claeys, M., Wildt, J., 2009. The formation, properties and impact of secondary organic aerosol: current and emerging issues. Atmos. Chem. Phys. 9 (14), 5155–5236.

Hawley, B., L'Orange, C., Olsen, D.B., Marchese, A.J., Volckens, J., 2014. Oxidative stress and aromatic hydrocarbon response of human bronchial epithelial cells exposed to petro- or biodiesel exhaust treated with a diesel particulate filter. Toxicol. Sci. 141 (2), 505–514. https://doi.org/10.1093/toxsci/kfu147.

HEI (Health Effects Institute), 2024: State of Global Air. Special Report. Boston, MA: Health Effects Institute. Online at https://www.stateofglobalair.org/resources/report/state-global-air-report-2024 (accessed 20 September 2024.

Hinds, W.C., 1999. Aerosol Technology: Properties, Behavior, and Measurement of Airborne Particles. John Wiley & Sons.

Hofmann, W., 2009. Modelling particle deposition in human lungs: modelling concepts and comparison with experimental data. Biomarkers 14 (sup1), 59–62. https://doi.org/10.1080/13547500902965120.

Holder, A.L., Lucas, D., Goth-Goldstein, R., Koshland, C.P., 2007. Inflammatory response of lung cells exposed to whole, filtered, and hydrocarbon denuded diesel exhaust. Chemosphere 70 (1), 13–19. https://doi.org/10.1016/j.chemosphere.2007.07.036.

Ihalainen, M., Jalava, P., Ihantola, T., Kasurinen, S., Uski, O., Sippula, O., Hartikainen, A., Tissari, J., Kuuspalo, K., Lahde, A., Hirvonen, M.R., Jokiniemi, J., 2018. Design and validation of an air-liquid interface (ALI) exposure device based on thermophoresis. Aerosol Sci. Tech. 53 (2), 1–13. https://doi.org/10.1080/02786826.2018.1556775.

Janssen, N.A., Hoek, G., Simic-Lawson, M., Fischer, P., van Bree, L., ten Brink, H., Keuken, M., Atkinson, R.W., Anderson, H.R., Brunekreef, B., Cassee, F.R., 2011. Black carbon as an additional Indicator of the adverse health effects of airborne particles compared with PM10 and PM2.5. Environ. Health Perspect. 119 (12), 1691–1699. https://doi.org/10.1289/ehp.1003369.

Krzyzanowski, M., Kuna-Dibbert, B., Schneider, J., 2005. Health Effects of Transport-Related Air Pollution. World Health Organization. Regional Office for Europe. https://iris.who.int/handle/10665/328088 (accessed 24 September 2024).

Künzli, N., Kaiser, R., Medina, S., et al., 2000. Public health impact of outdoor and traffic-related air pollution: a European assessment. Lancet 356, 895–901. https://doi.org/10.1016/S0140-6736(00)02653-2.

Lacroix, G., Koch, W., Ritter, D., et al., 2018. Air–liquid interface in vitro models for respiratory toxicology research: consensus workshop and recommendations. Appl. In Vitro Toxicol. 4 (2), 91–106. https://doi.org/10.1089/aivt.2017.0034.

Lawal, A.O., Zhang, M., Dittmar, M., Lulla, A., Araujo, J.A., 2015. Heme oxygenase-1 protects endothelial cells from the toxicity of air pollutant chemicals. Toxicol. Appl. Pharmacol. 284, 281–291. https://doi.org/10.1016/j.taap.2015.01.010.

Lelieveld, J., Haines, A., Burnett, R., Tonne, C., Klingmüller, K., Münzel, T., Pozzer, A., 2023. Air pollution deaths attributable to fossil fuels: observational and modelling study. Br. Med. J. 383, e077784. https://doi.org/10.1136/bmj-2023-077784.

Libalova, H., Rossner, P., Vrbova, K., et al., 2016. Comparative analysis of toxic responses of organic extracts from diesel and selected alternative fuels engine emissions in human lung BEAS-2B cells. Int. J. Mol. Sci. 17 (11), 1833. https://doi.org/10.3390/ijms17111833.

Martin, N., Lombard, M., Jensen, K.R., Kelley, P., Pratt, T., Traviss, N., 2017. Effect of biodiesel fuel on "real-world", nonroad heavy duty diesel engine particulate matter emissions, composition and cytotoxicity. Sci. Total Environ. 586, 409–418. https://doi.org/10.1016/j.scitotenv.2016.12.041.

Morin, J.P., Fouquet, F., Monteil, C., Le Prieur, E., Vaz, E., Dionnet, F., 1999. Development of a new in vitro system for continuous in vitro exposure of lung tissue to complex atmospheres: application to diesel exhaust toxicology. Cell Biol. Toxicol. 15 (30), 143–152. https://doi.org/10.1023/a:1007625302215.

Mülhopt, S., Dilger, M., Diabaté, S., Schlager, C., Krebs, T., Zimmermann, R., Buters, J., Oeder, S., Wäscher, T., Weiss, C., Paur, H.R., 2016. Toxicity testing of combustion aerosols at the air–liquid interface with a self-contained and easy-to-use exposure system. J. Aerosol Sci. 96, 38–55. https://doi.org/10.1016/j.jaerosci.2016.02.005.

Müller, L., Comte, P., Czerwinski, J., Kasper, M., Mayer, A.C., Gehr, P., Burtscher, H., Morin, J.P., Konstandopoulos, A., Rothen-Rutishauser, B., 2010. New exposure system to evaluate the toxicity of (scooter) exhaust emissions in lung cells in vitro. Environ. Sci. Technol. 44 (7), 2632–2638. https://doi.org/10.1021/es903146g.

Oberdörster, G., Sharp, Z., Atudorei, V., Elder, A., Gelein, R., Kreyling, W., Cox, C., 2004. Translocation of inhaled ultrafine particles to the brain. Inhal. Toxicol. 16, 437–445. https://doi.org/10.1080/08958370490439597.

Oeder, S., Kanashova, T., Sippula, O., et al., 2023. Particulate matter from both heavy fuel oil and diesel fuel shipping emissions show strong biological effects on human lung cells at realistic and comparable in vitro exposure conditions. PloS One 10 (6), e0126536. https://doi.org/10.1371/journal.pone.0126536.

Pozzer, A., Anenberg, S.C., Dey, S., Haines, A., Lelieveld, J., Chowdhury, S., 2023. Mortality attributable to ambient air pollution: a review of global estimates. GeoHealth 7 (1), e2022GH000711. https://doi.org/10.1029/2022GH000711.

Rössner Jr., P., Cervena, T., Vojtisek-Lom, M., et al., 2019. The biological effects of complete gasoline engine emissions exposure in a 3D human airway model (MucilAirTM) and in human bronchial epithelial cells (BEAS-2B). Int. J. Mol. Sci. 20 (22), 5710. https://doi.org/10.3390/ijms20225710.

Rössner Jr., P., Cervena, T., Vojtisek-Lom, M., 2021a. In vitro exposure to complete engine emissions–a mini-review. Toxicology 462, 152953.

Rössner, P., Cervena, T., Vojtisek-Lom, M., et al., 2021b. Markers of Lipid Oxidation and Inflammation in Bronchial Cells Exposed to Complete Gasoline Emissions and Their Organic Extracts. https://doi.org/10.1016/j.chemosphere.2021.130833.

Rössner, P., Libalova, H., Cervena, T., Sima, M., Simova, Z., Vrbova, K., Ambroz, A., Novakova, Z., Elzeinova, F., Vimrova, A., Dittrich, L., Vojtisek, M., Pechout, M., Vojtisek-Lom, M., 2024 Dec 7. Real-world outdoor air exposure effects in a model of the human airway epithelium - A comparison of healthy and asthmatic individuals using a mobile laboratory setting. Ecotoxicol. Environ. Saf. 289, 117495. https://doi.org/10.1016/j.ecoenv.2024.117495.

Rothen-Rutishauser, B., Blank, F., Mühlfeld, C., Gehr, P., 2008. In vitro models of the human epithelial airway barrier to study the toxic potential of particulate matter. Expert Opin. Drug Metab. Toxicol. 4 (8), 1075–1089. https://doi.org/10.1517/17425255.4.8.1075.

Saveleva, L., Cervena, T., Mengoni, C., et al., 2024. Transcriptomic and epigenomic profiling reveals altered responses to diesel emissions in Alzheimer's disease both in vitro and in population-based data. Alzheimers Dement., 14347 https://doi.org/10.1002/alz.14347.

Savi, M., Kalberer, M., Lang, D., Ryser, M., Fierz, M., Gaschen, A., Ricka, J., Geiser, M., 2008. A novel exposure system for the efficient and controlled deposition of aerosol particles onto cell cultures. Environ. Sci. Technol. 42 (15), 5667–5674. https://doi.org/10.1021/es703075q.

Steiner, S., Mueller, L., Popovicheva, O.B., Raemy, D.O., Czerwinski, J., Comte, P., Mayer, A., Gehr, P., Rothen-Rutishauser, B., Clift, M.J., 2012. Cerium dioxide nanoparticles can interfere with the associated cellular mechanistic response to diesel exhaust exposure. Toxicol. Lett. 214 (2), 218–225. https://doi.org/10.1016/j.toxlet.2012.08.026.

Steiner, S., Heeb, N.V., Czerwinski, J., Comte, P., Mayer, A., Petri-Fink, A., Rothen-Rutishauser, B., 2014. Test-methods on the test-bench: a comparison of complete exhaust and exhaust particle extracts for genotoxicity/mutagenicity assessment. Environ. Sci. Technol. 48 (9), 5237–5244. https://doi.org/10.1021/es4056033.

Steiner, S., Czerwinski, J., Comte, P., Heeb, N.V., Mayer, A., Petri-Fink, A., Rothen-Rutishauser, B., 2015. Effects of an iron-based fuel-borne catalyst and a diesel particle filter on exhaust toxicity in lung cells in vitro. Anal. Bioanal. Chem. 407 (20), 5977–5986. https://doi.org/10.1007/s00216-014-7878-5.

Stolcpartova, J., Pechout, M., Dittrich, L., Mazac, M., Fenkl, M., Vrbova, K., Ondracek, J., Vojtisek-Lom, M., 2015. Combustion engines as the main source of ultrafine particles in residential neighborhoods: field measurements in the Czech Republic. Atmosphere 6 (11), 1714–1735. https://doi.org/10.3390/atmos6111714.

Tippe, A., Heinzmann, U., Roth, C., 2002. Deposition of fine and ultrafine aerosol particles during exposure at the air/cell interface. J. Aerosol Sci. 33 (2), 207–218. https://doi.org/10.1016/S0021-8502(01)00158-6.

Totlandsdal, A.I., Lag, M., Lilleaas, E., Cassee, F., Schwarze, P., 2015. Differential proinflammatory responses induced by diesel exhaust particles with contrasting PAH and metal content. Environ. Toxicol. 30 (2), 188–196. https://doi.org/10.1002/tox.21884.

Upadhyay, L. Palmberg, Air-liquid interface: relevant in vitro models for investigating air pollutant-induced pulmonary toxicity, Toxicol. Sci. 164 (2018) 21–30. doi:https://doi.org/10.1093/toxsci/kfy053.Vojtisek-Lom, M., Pechout, M., Macoun, D., Rameswaran, R., Praharaj, K. K., Cervena, T., … & Rossner, P. (2019). Assessing exhaust toxicity with biological detector: configuration of portable air-liquid interface human lung cell model exposure system, sampling train and test conditions. SAE International Journal of Advances and Current Practices in Mobility, 2(2019-24-0050), 520–534.

Vojtisek-Lom, M., Pechout, M., Macoun, D., Rameswaran, R., et al., 2020. Assessing exhaust toxicity with biological detector: configuration of portable air-liquid interface human lung cell model exposure system, sampling train and test conditions. SAE Int. J. Adv. & Curr. Prac. in Mobility 2 (2), 520–534. https://doi.org/10.4271/2019-24-0050.

Vu, T.V., Ondracek, J., Zdímal, V., Schwarz, J., Delgado-Saborit, J.M., Harrison, R.M., 2017. Physical properties and lung deposition of particles emitted from five major indoor sources. Air Qual. Atmos. Health 10, 1–14.

WHO (World Health Organization), 2021. WHO global air quality guidelines: particulate matter (PM2.5 and PM10), ozone, nitrogen dioxide, sulfur dioxide and carbon monoxide. https://www.who.int/publications/i/item/9789240034228 (accessed 23 September 2024).

Zavala, J., Lichtveld, K., Ebersviller, S., Carson, J.L., Walters, G.W., Jaspers, I., Jeffries, H.E., Sexton, K.G., Vizuete, W., 2014. The Gillings sampler-an electrostatic air sampler as an alternative method for aerosol in vitro exposure studies. Chem. Biol. Interact. 220, 158–168.

Zhang, Z.-H., Balasubramanian, R., 2014. Physicochemical and toxicological characteristics of particulate matter emitted from a non-road diesel engine: comparative evaluation of biodieseldiesel and butanol-diesel blends. J. Hazard. Mater. 264, 395–402. https://doi.org/10.1016/j.jhazmat.2013.11.033.